

FPGA-based on-line Neural Network in Energy Storage System for Power Regulation of Wind-turbine Generator

Y.Y. Hong Y.T. Ye Y.R. Chang Y.D. Lee P.W. Liu

Abstract-- Stochastic characteristics of wind power generation may lead to reliability and power quality problems in power systems. This paper presents two control schemes considering state-of-charge (SOC) in the energy storage system for the wind-turbine-generator: constant power mode and power balance mode. Because the response of energy storage system is not fast enough, estimated coming wind power is gained by wind speed forecasting for the charging/discharging control applied to the energy storage system. An on-line learning algorithm is developed in an Elman-based recurrent neural network implemented in the power balance mode to conduct the wind speed forecasting several minutes ahead. This paper uses a Real-time Digital Simulator (OPAL-Lab OP5600) to investigate the performance of the proposed method. The on-line learning Elman-based recurrent neural network is implemented by a Xilinx FPGA. The wind-turbine-generator, power converters, energy storage, resistance load and the power grid are modeled in the Real-time Digital Simulator using SIMULINK/ARTEMIS. Thus, a co-simulation (i.e., FPGA-in-the-loop simulation) is developed in this work. The ratio of CPU times required to study a scenario by a regular PC, Windows Target, and OPAL-Lab on the average is about 14.2: 1.87: 1. The studied results obtained from this FPGA-in-the-loop simulation verify the applicability of the proposed method.

Keywords: On-line learning, wind power, forecasting, real-time simulation, FPGA.

I. INTRODUCTION

DISTRIBUTED Generation (DG, e.g., wind farm, photovoltaic array, fuel cell and micro-turbine, etc.) has attracted increasing attention due to its significant impact on environment and mitigation of greenhouse gas emission. Especially, there are many commercial products, which can provide larger real power from the wind-turbine-generators in the power system. However, the stochastic characteristics of wind power generation lead to reliability and power quality problems in power systems. To help improve the operational problem caused by intermittent characteristics of wind power generations, many methods were proposed to implement the

energy storage system to regulate the power fluctuation. Essentially, these methods were classified into two categories: steady-state and dynamic studies.

For the steady-state studies, Wang et al. proposed a technique to evaluate operational reliability and energy utilization efficiency of power systems with high wind power penetration [1]. The ramp rate of a conventional generator and energy storage system were considered. The impact of slow ramp-up rate or fast reduction of wind speed on system reliability is measured by the expected energy not supplied. Ghofrani et al. dealt with optimal placement of the energy storage units within a deregulated power system to minimize its hourly social cost [2]. Wind generation and load are modeled using probabilities for utilizing probabilistic optimal power flow (POPF) to maximize wind power utilization over a scheduling period. Hartmann and Dán proposed two different complementary methods to determine the parameters (rated power and energy) of a grid-connected energy storage unit that is capable of providing auxiliary control reserves required by wind power plants where the power system may be partially or wholly not capable of operation [3]. Wee et al. designed a battery-supercapacitor energy storage system for a wind farm [4]. By treating the input wind power as a random variable and using a proposed coordinated power flows control strategy for the battery and the supercapacitor, the proposed method evaluated the energy storage capacities and the expected cost/year of unmet power dispatch. Ghofrani et al. presented a genetic algorithm-based approach together with a probabilistic optimal power flow to optimally place and adequately size the energy storage [5]. The proposed method minimized the sum of operation and interrupted-load costs over a planning period.

The dynamic studies, on the other hand, addressed dynamic/real-time simulation and control strategies. Brekken et al. proposed sizing and control methodologies for an energy storage system based on artificial neural network control strategies which resulted in significantly lower cost energy storage systems than simplified controllers [6]. Jiang et al. proposed a battery energy storage system using a dual-layer control strategy consisting of a fluctuation mitigation control layer and a power allocation control layer to mitigate wind farm power output fluctuations [7]. This method combined both dynamic control and steady-state mixed-integer quadratic programming. Lee et al. proposed a method to compensate the output of Cheju Island's Heangwon wind farm by utilizing (i) a superconducting flywheel, which has a quick response and low power capacity, and (ii) a battery energy storage system, which has a comparatively lower response capability and high power capacity [8]. Jiang and Hong presented a wind power filtering approach to mitigate short- and long-term fluctuations

This work was supported by the Ministry of Science and Technology under the grant number MOST 104-3113-E-042A-004-CC2.

Y.Y. Hong is with Dept. of EE, Chung Yuan Christian University (CYCU), Taoyuan City 32023 Taiwan. (e-mail of corresponding author: yyhong@dec.ee.cycu.edu.tw).

Y.T. Ye is graduate student at CYCU. (e-mail: tp90133@gmail.com).

Y.R. Chang is with Institute of Nuclear Energy Research (INER), Longtan, Taiwan. (email: raymond@iner.gov.tw)

Y.D. Lee is with INER, Longtan, Taiwan. (email: ydllee@iner.gov.tw)

P.W. Liu is with INER, Longtan, Taiwan. (email: wayne@iner.gov.tw)

Paper submitted to the International Conference on Power Systems Transients (IPST2015) in Cavtat, Croatia June 15-18, 2015

using a hybrid energy storage system sized by a novel wavelet-based capacity configuration algorithm [9, 10]. An ultra-capacitor bank mitigated short-term fluctuations and a lithium-ion battery bank minimized long-term fluctuations. Delille et al. presented a dynamic approach to study the provision of a dynamic frequency control supported by energy storage systems while considering large wind or solar generations [11]. The results showed that fast-acting storage, like a synthetic inertia, can mitigate the impact of these sources in case of a major generation outage. Islam et al. presented a control scheme combined with short-term wind speed prediction for management of the stored energy in a small capacity flywheel energy storage system which was used to mitigate the output power fluctuations of an aggregated wind farm [12]. In this study, a wind speed prediction was conducted by artificial neural network, which was developed in MATLAB/Simulink and interfaced with PSCAD/EMTDC.

This paper presents two control modes considering state-of-charge (SOC) in the energy storage system for the wind-turbine-generator: constant power mode and power balance mode. Because the response of energy storage system is not fast enough, estimated coming wind power is gained by wind speed forecasting for the charging/discharging controls applied to the energy storage system. An on-line learning algorithm is developed in an Elman-based recurrent neural network implemented in the control schemes to conduct the wind speed forecasting several minutes ahead. This paper uses a Real-time Digital Simulator (OPAL-Lab OP5600) to investigate the performance of the proposed method. The on-line learning Elman-based recurrent neural network is implemented by a Xilinx FPGA (Field-Programmable Gate Arrays). The wind-turbine-generator, power converters, energy storage, resistance load and the power grid are modeled in the Real-time Digital Simulator using SIMULINK/ARTEMIS. The tests are conducted by a co-simulation (i.e., FPGA-in-the-loop simulation) in this work.

II. PROPOSED METHOD

As described in Sec. I., the energy storage system is placed at the DC bus to perform the constant power mode and power balance mode, as shown in Fig. 1. The wind turbine provides a torque to the permanent magnetic synchronous generator (PMSG). Fig. 2 illustrates the control module consists of these two modes with the input of SOC (state-of-charge) measurement from the energy storage. The control module receives either a constant power setting or load value for balancing, in addition to forecasted wind power generation. The MK ES10-12S Pb-acid batteries (600V, 833Ah) are modeled herein. The numbers of series and parallel batteries are 12 and 83, respectively. The SOC is operated within 20%~85% [13] for prolonging the life of the batteries.

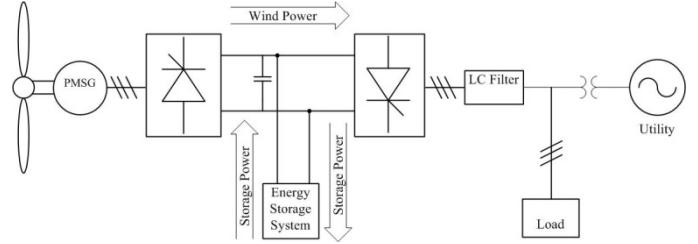


Fig. 1. The studied system.

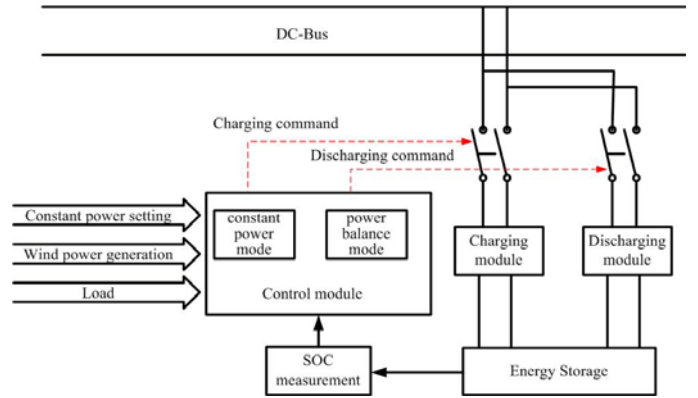


Fig. 2. The control, charging, discharging, and measurement modules.

Because the response of energy storage system is not fast enough, estimated coming wind power, applied to the energy storage system only in the power balance mode, is acquired by the wind speed forecasting result. An on-line learning algorithm is developed in an Elman-based recurrent neural network to conduct the wind speed forecasting several minutes ahead.

A. On-line Learning in Recurrent Neural Network

The wind speeds $S(t-1)$, $S(t-2)$ and $S(t-3)$ are used to forecast $S(t)$ in this paper using the Elman-based recurrent neural network, as shown in Fig. 3. The weighting factors and biases (thresholds) are acquired when the off-line training iterations converge using MATLAB. Table 1 shows the definitions of variables in MATLAB. The convergent values of these variables serve as initial conditions for on-line learning algorithm while on-line conditions are concerned.

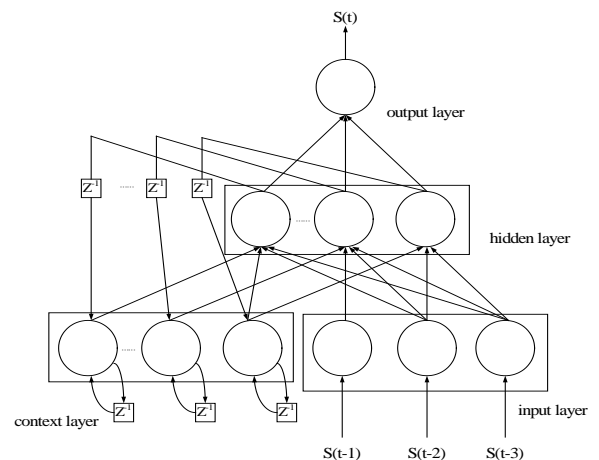


Fig.3. Recurrent neural network for wind speed forecasting.

TABLE I
DEFINITIONS OF VARIABLES IN MATLAB.

Variables in MATLAB	Definitions
IW1,1	Weighting factors in input layer
LW1,1	Weighting factors in recurrent layer
LW2,1	Weighting factors in output layer
B1	Bias (threshold) in input layer
B2	Bias (threshold) in output layer

In this paper, only the weighting factors and biases in the output layer are updated on-line. Let the activation function in the output layer be hyperbolic tangent as follows.

$$f(\varphi) = y = \frac{1}{1+e^{-\varphi}} \quad (1)$$

Compute the derivative of (1):

$$\frac{d}{d\varphi} f(\varphi) = \frac{e^{-\varphi}}{(1+e^{-\varphi})^2} = (y-1)y^2 \quad (2)$$

Let the input values and the bias in the output layer be:

$$X = [x_1, x_2, \dots, x_n, -1] \quad (3)$$

and the weighting factors and coefficient of the bias be

$$W = [w_1, w_2, \dots, w_n, b] \quad (4)$$

Then the output can be expressed as follows:

$$\varphi = W \cdot X^T = w_1 \times x_1 + w_2 \times x_2 + \dots + w_n \times x_n - b \quad (5)$$

$$\text{Then } \frac{\partial \varphi}{\partial w_i} = x_i, i = 1, 2, \dots, n \quad (6)$$

and

$$\frac{\partial \varphi}{\partial b} = -1 \quad (7)$$

Let y^* be known. If the error function $E(e)=e^2/2=(y^*-y)^2/2$, then

$$\frac{\partial E(e)}{\partial w_j} = e \cdot \frac{\partial e}{\partial w_j} = -e \cdot \frac{dy}{d\varphi} \cdot \frac{\partial \varphi}{\partial w_j} = -e \cdot (y-1) \cdot y^2 \cdot x_j \quad (8)$$

$$\frac{\partial E(e)}{\partial b} = e \cdot \frac{\partial e}{\partial b} = -e \cdot \frac{dy}{db} \cdot \frac{\partial \varphi}{\partial b} = e \cdot (y-1) \cdot y^2 \quad (9)$$

Equations (8) and (9) are used to serve as Δw_j and Δb to update the weighting factor w_j and bias b in the output layer on-line [14]. When the wind speed $S(t)$ is forecasted using $S(t-1)$, $S(t-2)$ and $S(t-3)$, the wind power generation at time t is estimated using Fig. 4. This wind power generation serves as an input to the control module, as shown in Fig. 2.

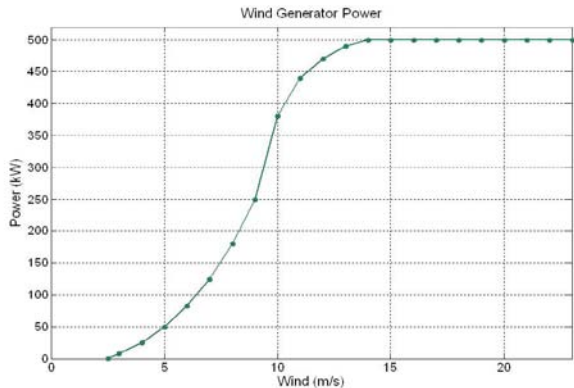


Fig. 4. kW vs. m/s for a 500kW PMSG.

B. Constant Power Mode and Power Balance Mode

In the constant power mode, the PMSG is operated with the maximum power point tracking (MPPT) or user-defined kW which is smaller than that controlled by MPPT. If the energy storage is operated in the constant power mode, then the total output from both the wind power and energy storage is fixed at a specified value, e.g., 500 kW. The control logic for the power balance mode of the energy storage is shown in Fig. 5. If the value of SOC within its specified limits, then two “0” are sent to XNOR. If $W \geq C$, then “AND gate 1” outputs “1” enabling the charging action. This paper implements 10A in the constant current charging mode. On the contrary, If $W < C$, then “AND gate 2” outputs “1” enabling the constant-voltage discharging action. If the SOC is smaller than its low limit, the charging mode is activated. The voltage of DC bus should follow the curve given in Fig. 6 in order to compensate the insufficient power between the wind-turbine generator and the demand.

In the power balance mode, the wind power generation is forecasted and the level of load is known. The control logic is similar to that in Fig. 5, except for the “Constant kW setting” replaced by “Constant total power.” Fig. 7 shows the kW generation from energy storage vs. the DC voltage.

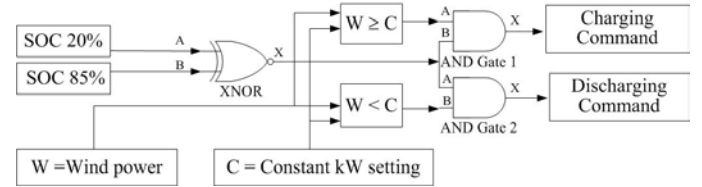


Fig. 5. Control logic of constant power mode.

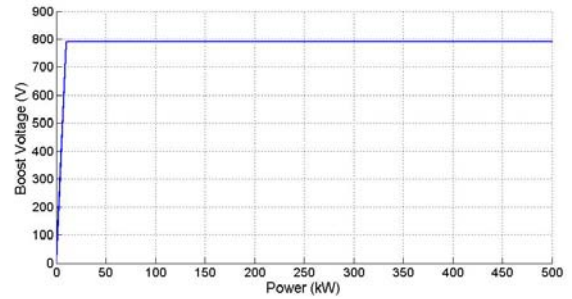


Fig. 6. Power generation vs. DC voltage in the constant power mode.

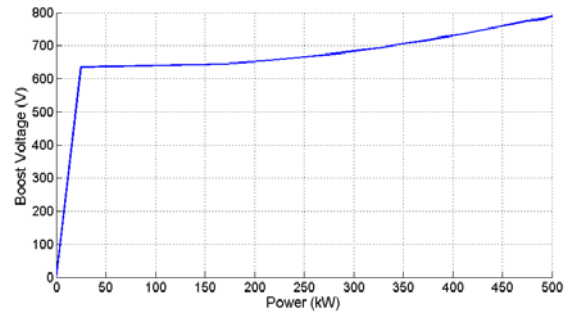


Fig. 7. Power generation vs. DC voltage in the power balance mode.

C. Real-time Digital Simulator

To implement the proposed method, a real-time simulation approach using eMegaSim for the studied system

in Fig. 1 is presented in this work. The eMegaSim developed by Opal-RT Technologies Inc. is utilized by a host computer and a target computer with 4 cores in one CPU [15]. The eMegaSim consisting of software (RT-Lab) and hardware (target computer OP5600; Inter(R) i686 3.3GHz, 4.0GB RAM) can be completely integrated with the SIMULINK/ARTEMIS. The user can develop his SIMULINK/ARTEMIS code in a host PC (Intel(R) Core(TM)2 Quad CPU Q9400 2.6GHz, 3.25GB RAM herein) first. The parallel computation was realized in Opal-RT-Redhat OS. The Simulink-based code is then moved to the Opal-RT-Redhat OS to achieve parallel computation in the target computer.

A powerful FPGA is included in OP5600. A Xilinx ML605 development board, which is based on the Xilinx Virtex-6 CX6VLX240T processor, is used for floating-point models and projects requiring the use of large amounts of on-board memory. In this paper, Xilinx System Generator (ISE 12.3) for DSP is used to design both the on-line learning algorithm and the neural network. The other parts of the studied system (e.g., PMSG, AC/DC converter, DC/AC converter, energy storage system, filter, load, and utility system) are modeled by using SIMULINK/ARTEMIS. Fig. 8 shows the on-line learning algorithm developed using Xilinx System Generator.

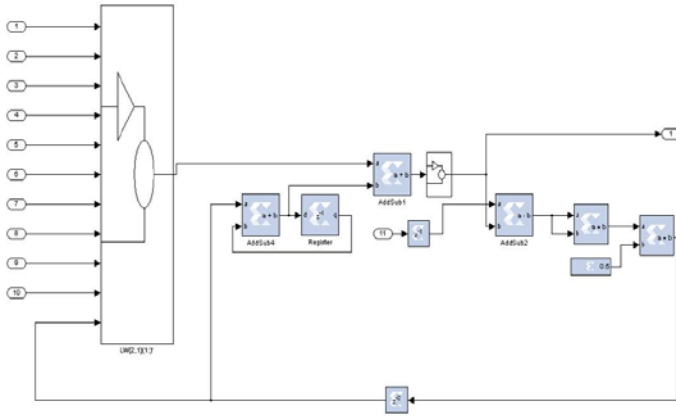


Fig. 8. Modularized on-line learning algorithm using Xilinx System Generator.

III. TEST RESULTS

The studied system is shown in Fig. 1. This system includes a PMSG whose rate voltage and capacity are 380 V and 500 kVA, respectively. The cut-in and cut-off wind speeds are 2.5 and 24 m/s, respectively. The Pb-Acid energy battery system is operated at 600 V and 833Ah. The utility side is operated at 11.4 kV, 40 MVA (short circuit capacity) and $X/R=7$.

A. Scenario 1- Constant Power Mode with Decreasing Wind Speed

In this scenario, the total kW generation from the energy storage system and wind-turbine generator is 500 kW in case of $20\% \leq \text{SOC} \leq 85\%$. The variation of wind speed is shown in Fig. 9. If the wind speed exceeds 14 m/s, the wind-turbine generator produces 500 kW which charges the batteries;

otherwise, the energy storage discharges. Figs. 10 and 11 illustrate the variations of SOC and kW/kVAR, respectively. It can be found that the kW from the energy storage can compensate the shortage of wind power.

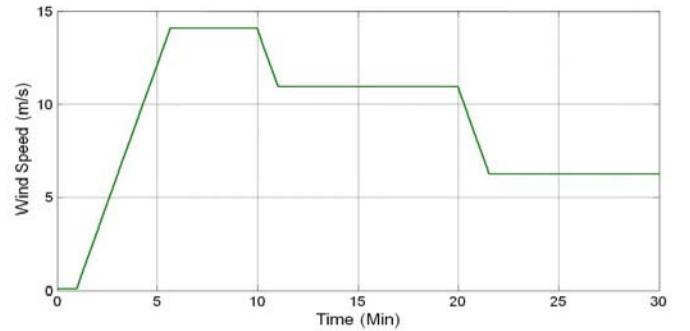


Fig. 9. Variation of wind speed in Scenario 1.

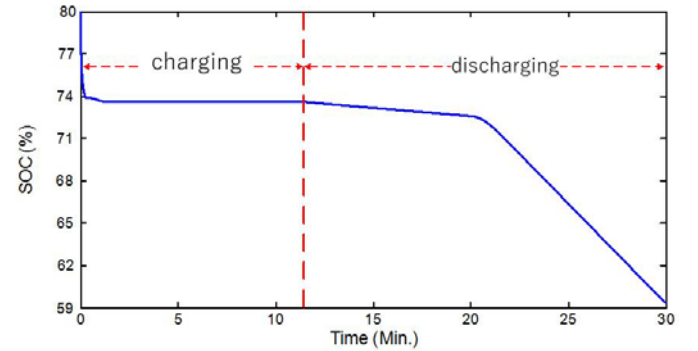


Fig. 10. Variation of SOC in Scenario 1.

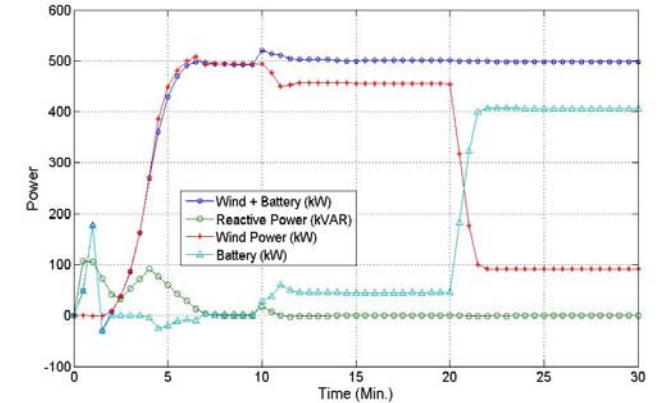


Fig. 11. Variations of kW/kVAR in Scenario 1.

B. Scenario 2- Constant Power Mode with Increasing Wind Speed

Scenario 2 shows the energy storage system is operated with the constant power mode while the wind speed is increasing, as shown in Fig. 12. Due to the wind speed, the energy storage discharges ($S(t) \leq 14$ m/s) before 20 minutes and charges ($S(t) > 14$ m/s) after 20 minutes, as shown in Fig. 13. Fig. 14 gives the variations of kW/kVAR in all devices. It can be found that 500-kW generation from the energy storage and wind-turbine generator still remains.

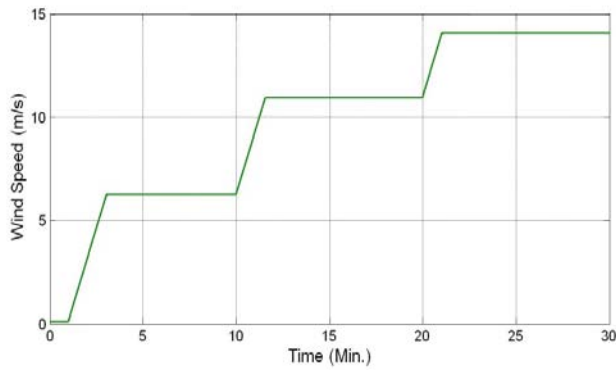


Fig. 12. Variation of wind speed in Scenario 1.

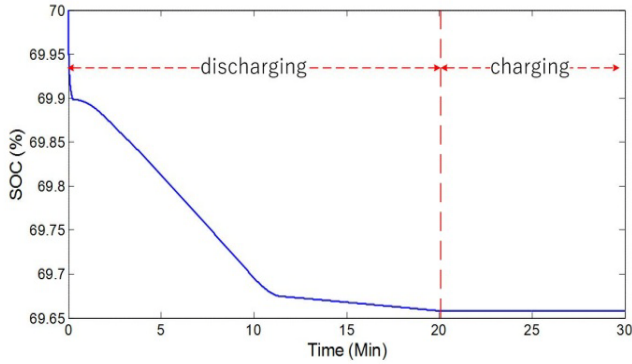


Fig. 13. Variation of SOC in Scenario 1.

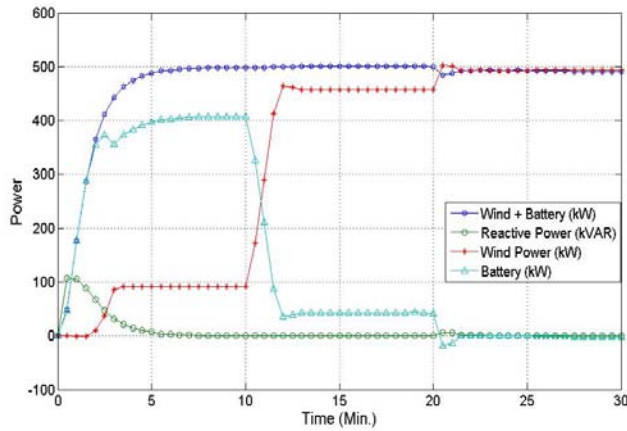


Fig. 14. Variations of kW/kVAR in Scenario 2.

C. Scenario 3- Power Balance Mode with Adequate Wind

In the power balance mode, the on-line learning algorithm is used to forecast the future wind speed which is used to evaluate the wind power generation. The time interval is 17 minutes; that's, the wind speeds at $t=0, 17, 34$ minutes are utilized to forecast that at $t=51$ minutes.

Fig. 15 shows the wind speeds are within 4-8 m/s which is corresponding to 30-180kW. Fig. 16 illustrates the variation of SOC. In this scenario, the load is 300 kW. Before $t=51$ minutes, the wind power is not forecasted and the wind power generation is smaller than the load; consequently, the energy storage provides inadequate power during this interval. After $t=51$ minutes, the evaluated wind power incorporating with the neural network forecasting is smaller than the load; thus, the energy storage still discharges. Fig. 17 shows the variations of kW/kVAR in Scenario 3.

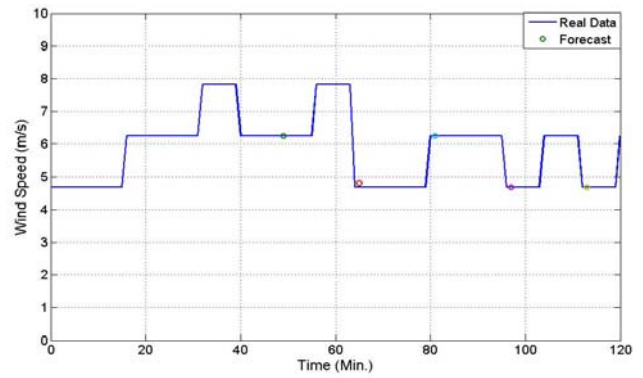


Fig. 15. Variation of wind speed in Scenario 3.

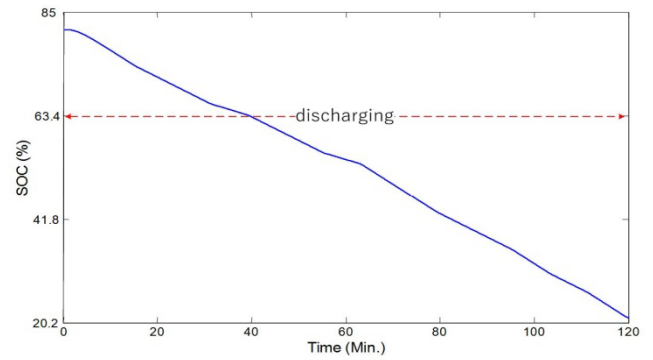


Fig. 16. Variation of SOC in Scenario 3.

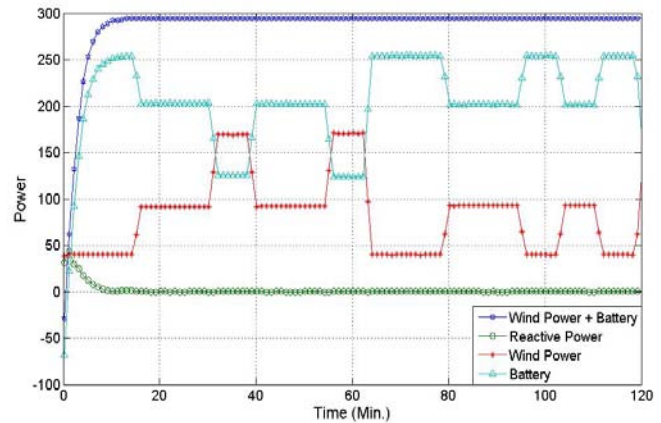


Fig. 17. Variations of kW/kVAR in Scenario 3.

D. Scenario 4- Power Balance Mode with Abounding Wind

Fig. 18 shows the wind speeds are within 3-14 m/s which corresponds to 20-500kW. Fig. 19 illustrates the variation of SOC.

Before $t=51$ minutes, no forecasted wind speed/power are available. In case the wind power generation exceeds the demand, the energy storage is standby; otherwise, the energy storage compensates the inadequate amount from the wind power.

After $t=51$ minutes, if the output of the neural network implies that the evaluated wind power is smaller than the demand, the energy storage discharges; otherwise charges. The wind power plus the energy storage power retains 350 kW (level of load in this scenario). Near $t=91$ minutes, the wind power is much greater than the load and the power system receives the excess power, as shown in Fig. 20.

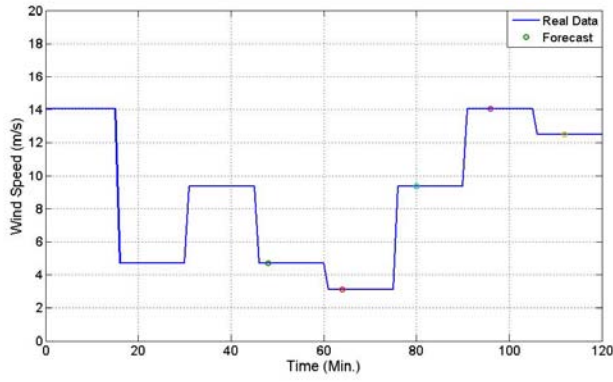


Fig. 18. Variation of wind speed in Scenario 4.

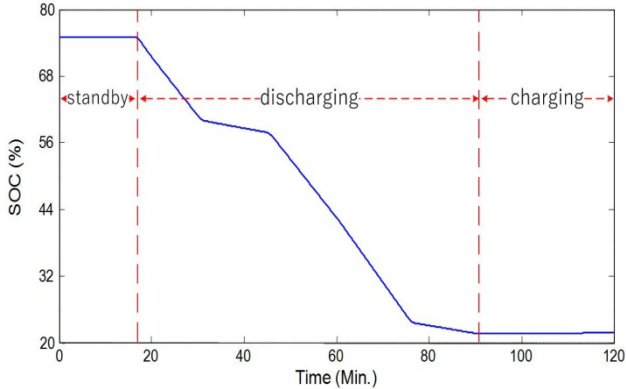


Fig. 19. Variation of SOC in Scenario 4.

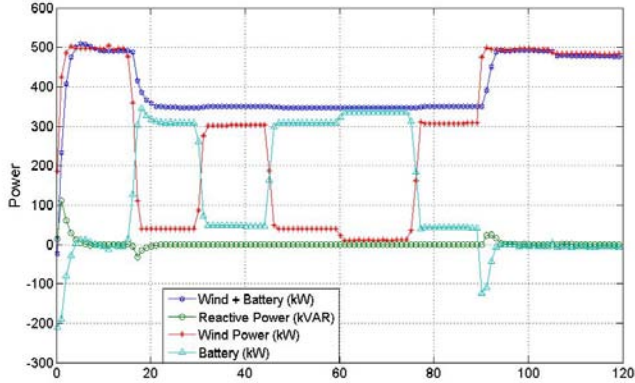


Fig. 20. Variations of kW/kVAR in Scenario 4.

E. Simulation Times

In this paper, the Opal-RT OP5600 is adopted to study the above FPGA-in-the-loop simulation. The OP5600 has four 3.3-GHz processor cores with the real-time operating system of QNX and Red Hat Linux. For comparative studies, the Window Target and regular PC are used to study the same scenarios. The sampling rate is $10 \mu\text{s}$ and ODE3 algorithm for solving differential equations is used. Due to the long elapsed time required, the simulation time is scaled down to 1/60. For example, realistic 30 minutes will be simulated in 30 seconds. Table II shows the CPU times required in all simulations. Please note that Window target and regular PC cannot conduct the FPGA-in-the-loop simulation; that's, the neural network is realized by SIMULINK. It can be found that the OP5600 conducts the real-time simulation but both Window Target and regular PC require long CPU times. For

scenario 1, the ratio of CPU times required by a regular PC, Windows Target, and OPAL-Lab on the average is 14.2: 1.87: 1. Table III shows the resources used in the developed FPGA in Opal-RT OP5600. The operating frequency of the FPGA is 13.785MHz.

TABLE II
COMPARATIVE STUDIES USING DIFFERENT SIMULATION TOOLS.

Scenarios	Simulation time	Simulation tool	CPU times (s)
Scenario 1	30 min	RT-Lab	29.97
		Windows Target	56
		Regular PC	427
Scenario 2	30 min	RT-Lab	29.97
		Windows Target	57
		Regular PC	434
Scenario 3	120 min	RT-Lab	119.88
		Windows Target	231
		Regular PC	2697
Scenario 4	120 min	RT-Lab	119.88
		Windows Target	499
		Regular PC	2732

TABLE III
RESOURCES USED IN XILINX VIRTEX-6 CX6VLX240T FPGA

Items	Utilizations
Number of Slice Registers	971 out of 301440
Number of Slice LUTs	23773 out of 150720
Number used as Logic	23757 out of 150720
Number used as Memory	16 out of 58400
Number of Flip Flops	23773 out of 24744
Number of LUT	971 out of 24744
Number of DSP48E1s	762 out of 768

IV. CONCLUSIONS

In this paper, two control modes developed in an energy storage system are presented for power regulations of a grid-connected wind-turbine generator. The power balance mode tends to compensate the inadequate power caused by the intermittent wind power to the local load while the constant power mode conducts a fixed power generation from both wind-turbine and energy storage. The Xilinx Virtex-6 CX6VLX240T FPGA in Opal-RT OP5600 is utilized to implement the on-line learning algorithm and recurrent neural network to forecast the wind power/speed. The proposed method is validated with test results based on FPGA-in-the-loop simulations by using the real-time Opal-Lab simulator. From the simulations, it can be found the proposed method can efficiently regulate the specified power in different wind speed conditions. Moreover, the developed FPGA can be implemented for realistic applications.

V. ACKNOWLEDGMENT

The authors gratefully acknowledge the financial support from the Ministry of Science and Technology in Taiwan under the grant number MOST 104-3113-E-042A-004 -CC2.

VI. REFERENCES

- [1] P. Wang, Z.Y. Gao, and L.B. Tjernberg, "Operational adequacy studies of power systems with wind farms and energy storages," IEEE Trans. on Power

Systems, vol. 27, no. 4, pp. 2377-2384, Nov. 2012.

[2] M. Ghofrani, A. Arabali, M. Etezadi-Amoli, and M.S. Fadali, "A framework for optimal placement of energy storage units within a power system with high wind penetration," *IEEE Trans. on Sustainable Energy*, vol. 4, no. 2, pp. 434-442, Apr. 2013.

[3] B. Hartmann and A. Dán, "Methodologies for storage size determination for the integration of wind power," *IEEE Trans. on Sustainable Energy*, vol. 5, no. 1, pp. 182-189, Jan. 2014.

[4] K.W. Wee, S.S. Choi, and D. M. Vilathgamuwa, "Design of a least-cost battery-supercapacitor energy storage system for realizing dispatchable wind power," *IEEE Trans. on Sustainable Energy*, vol. 4, no. 3, pp. 786-196, July 2013.

[5] M. Ghofrani, A. Arabali, M. Etezadi-Amoli, and M. S. Fadali, "Energy storage application for performance enhancement of wind integration," *IEEE Trans. on Power Systems*, vol. 28, no. 4, pp. 4803-4811, Nov. 2013.

[6] T.K.A. Brekken, A. Yokochi, A. von Jouanne, Z.Z. Yen, H.M. Hapke, and D.A. Halamay, "Optimal energy storage sizing and control for wind power applications," *IEEE Trans. on Sustainable Energy*, vol. 2, no. 1, pp. 69-77, Jan. 2011.

[7] Q.Y. Jiang, Y.Z. Gong, and H.J. Wang, "A battery energy storage system dual-layer control strategy for mitigating wind farm fluctuations," *IEEE Trans. on Power Systems*, vol. 28, no. 3, pp. 3263-3263, Aug. 2013.

[8] H. Lee, B.Y. Shin, S. Han, S. Jung, B. Park, and G. Jang, "Compensation for the power applications," *IEEE Trans. on Applied Superconductivity*, vol. 22, no. 3, June 2012.

[9] Q.Y. Jiang and H.S. Hong, "Wavelet-based capacity configuration and coordinated control of hybrid energy storage system for smoothing out wind power fluctuations," *IEEE Trans. on Power Systems*, vol. 28, no. 2, pp. 1363-1369, May 2013.

[10] Q.Y. Jiang and H.J. Wang, "Two-time-scale coordination control for a battery energy storage system to mitigate wind power fluctuations," *IEEE Trans. on Energy Conversion*, vol. 28, no. 1, pp. 52-61, Mar. 2013.

[11] G. Delille, B. François, and G. Malarange, "Dynamic frequency control support by energy storage to reduce the impact of wind and solar generation on isolated power system's inertia," *IEEE Trans. on Sustainable Energy*, vol. 3, NO. 4, pp. 931-939, Oct. 2012.

[12] F. Islam, A. Al-Durra and S.M. Mueeen, "Smoothing of wind farm output by prediction and supervisory-control-unit-based FESS," *IEEE Trans. on Sustainable Energy*, vol. 4, no. 4, pp. 925-933, Oct. 2013.

[13] N. Pinsky, J. Argueta, T. Knipe, V. Grosvenor, L. Gaillac, M. Merchant and A. Cabrera, "Fast charge of lead acid batteries at the SCE EV Tech Center," *The Fifteenth Annual Battery Conference on Applications and Advances*, pp.231-236, 11-14 Jan. 2000.

[14] W.M. Lin and C.M. Hong, "A New Elman Neural Network-Based Control Algorithm for Adjustable-Pitch Variable-Speed Wind-Energy Conversion Systems," *IEEE Trans. on Power Electronics*, vol. 26, no. 2, pp. 473-481, Feb. 2011.

[15] <http://opal-rt.com/>